



## Falsified medicines in Africa: all talk, no action

Poor-quality medicines and medical products, both substandard and falsified, cause avoidable morbidity, mortality, drug resistance, and loss of faith in health systems, especially in low-income and middle-income countries.<sup>1-3</sup> We report the analysis of two falsified medicines from Angola and discuss what lessons such a discovery could hold.

The tablets were seized at Luanda docks in June, 2012, after failing Minilab testing.<sup>4,5</sup> The seized shipment was enormous (1·4 million packets), and hidden in loudspeakers in a container from China.<sup>4</sup> One sample was labelled as an adult course of the vital antimalarial drug artemether-lumefantrine, and as being manufactured by "Novartis Pharmaceutical Corporation"; it also bore an Affordable Medicines Facility—malaria logo (figure). Another sample was labelled as the broad-spectrum anthelmintic mebendazole, and as being manufactured by "Janssen-Cilag SpA".

We analysed the tablets with an array of analytical platforms, including high-performance liquid chromatography, ambient ionisation mass spectrometry, Raman spectroscopy, X-ray powder diffraction (XRD) analysis, nuclear magnetic resonance spectroscopy, isotope-ratio mass spectrometry (IRMS), and botanical assays. Packaging was analysed with the portable counterfeit detection device CD-3 (see appendix for detailed methods).

No artemether, lumefantrine, or other active pharmaceutical ingredients were detected in the "artemether-lumefantrine" tablets by any of the chemical assay techniques. Brushite and three different yellow dyes (pigment yellow 3, pigment yellow 81, and pigment yellow 151) were detected. No mebendazole was detected in the "mebendazole" tablets, but the active ingredient levamisole (270 mg/tablet) was. XRD analysis revealed the presence of calcite

(CaCO<sub>3</sub>), with IRMS data suggesting that it was either hydrothermal or medical in origin. The CD-3 ultraviolet-visible and infrared images of the falsified and genuine packaging readily showed substantial differences between them. Language errors on the "mebendazole" packages were common, suggesting that the forger may have had some knowledge of English but little of French and Spanish.

Falsified artemether-lumefantrine has also been described across central and west Africa.<sup>5</sup> Such products will inevitably cause increased morbidity, mortality, and transmission, and could falsely indicate that artemisinin resistance had arrived. Additionally, modelling strongly suggests that underdosing is an important contributor to resistance.<sup>6</sup> Therefore, if patients consume co-circulating falsified and substandard medicines sequentially, so that heavy parasite burdens encounter low drug concentrations, the risks of engendering resistance are high.

The presence of the anthelmintic levamisole is also worrying because it has been withdrawn from many markets for human use owing to its association with agranulocytosis. The recent epidemic of necrotising vasculitis resulting from "cutting" cocaine with levamisole<sup>7</sup> suggests links between criminals who produce narcotics and those who produce falsified medicines.

These examples illustrate the major obstacles to improving the global medicine supply. First, there is no global system for the mandatory reporting, assessment, and dissemination of information on suspicious medicines. The seizure in Angola was first brought to public attention on Facebook after 5 months, and in the printed press after 11 months.<sup>4</sup> It was Facebook who first alerted those responsible for malaria control liaison at WHO. Although such reporting is commendable, it is grossly inadequate for tropical public health what proportion of African malaria patients and their families reads Facebook and the *Wall Street Journal*? Until 2011–12 (when it was

invoked for the USA and EU), no nation had legislation requiring the pharmaceutical industry (which is often the first to know) to inform the relevant medicines regulatory authority (MRA) of drug falsification. It is extraordinary that, in 2014, such systems are widely in place for suspicious aircraft parts but not for suspicious medicines.<sup>8</sup> WHO's new Rapid Alert System facilitates information sharing on poor-quality medicines between medicines regulatory authorities (MRAs).<sup>5</sup> It should be mandatory and included in the International Health Regulations.<sup>1</sup> When pharmaceutical companies and others encounter suspicious medicines or medical products, there remains tension between commercial interests, the need to investigate, and the requirement to act quickly to safeguard public health. There is no consensus mechanism to adjudicate these decisions from a public health perspective. This stagnant system must change. All reports of suspect medicines known to the pharmaceutical industry and others should be reported to the WHO and MRA within 1 week for investigation, risk assessment, and appropriate dissemination. If those reporting wish delayed onward dissemination, an advisory committee of MRAs and WHO with independent advice should perform a rapid public health risk assessment. Compliance should be reported through a mechanism such as the Access to Medicine Index.

See Online for appendix

For the Access to Medicine Index see <http://www.accesstomedicineindex.org/>

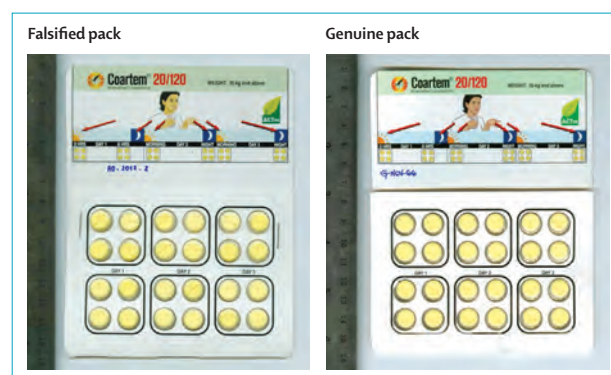


Figure: Scanned pictures of samples  
Top=falsified blister; bottom=genuine blister.

Second, recent inaction regarding medicine quality has involved disputes over definitions from a trade and political perspective. These disputes must have damaged public health. The acronym NATO (no action—talk only), sadly reflects recent history. Extended discussion at World Health Assemblies culminated in 2011 with the formation of a Member State mechanism. However, chairmanship disagreements then apparently delayed discussion for 6 months.<sup>9</sup> The group now has meetings just once per year.

The terminology remains confused—for example, a recent US Institute of Medicine report on medicine quality<sup>2</sup> did not state clearly what term should be used for medicines that are poor quality but not falsified. Here we have used the distinction between falsified (or counterfeit or spurious medicines—ie, those deliberately and fraudulently mislabelled with respect to identity or source) and substandard medicines (ie, genuine medicines produced by authorised manufacturers that do not meet quality specifications set for them by national standards).<sup>3</sup> To avoid any intellectual property connotations, the term falsified is used here instead of counterfeit.<sup>3</sup> We believe that this is the clearest way forward.

Third, the extradition and prosecution of criminals, such as those trading in falsified medicines between China and Angola, is extremely difficult as falsification of medicine or medical products is not an international crime, and definitions and laws are inconsistent. An international public health convention could assist in combating criminal networks and provide a financing mechanism for MRA and factory support (ie, detecting and reducing factory errors or negligence).<sup>3</sup> The Institute of Medicine favours soft-law solutions,<sup>2</sup> but the lack of legally binding force would neuter action.

Fourth, the enormous investment in accessible medicines and medical products without investment in checking their quality is profoundly illogical. WHO estimates that only

7% of sub-Saharan countries had a “moderately functioning MRA”.<sup>10</sup> We cannot expect the world’s medicine supply to improve without coordinated functional MRAs. They are essential for the interventions needed, and to ensure that the benefits of increased accessibility to free or inexpensive internationally financed medicines and inexpensive generics are translated effectively into improved public health. The Access to Medicines movement has been very important in improving access to essential medicines; however, much more emphasis is needed now on access to good quality medicines.

PN and NW are supported by Wellcome Trust of Great Britain. FMF would like to thank the NSF MRI grant #0923179 and the NSF/NASA Center for Chemical Evolution CHE-1004570 for the use of equipment acquired under these projects, and the GT School of Chemistry and Biochemistry for a Vasser-Wooley faculty fellowship that provided resources for this work. PD and MJC were supported by the ACT Consortium via an award from the Bill & Melinda Gates Foundation to the London School of Hygiene and Tropical Medicine. PT was supported by the Institut de Recherche sur l’Asie du Sud-Est Contemporaine (IRASEC) through funding from the French Ministry of Foreign and European Affairs (FSP Mekong Project). We are extremely grateful to the US Food and Drug Administration and to Nicola Ranieri for lending a CD-3 device and for all their assistance. We thank David Hawksworth and Patricia Wiltshire for the identification of fungal spores, Mayfong Mayxay for “NATO”, and Johnson & Johnson Companies and Novartis International AG for their assistance. We declare no competing interests.

Copyright © Newton et al. Open access article published under the terms of CC BY.

\*Paul N Newton, Patricia Tabernero, Prabha Dwivedi, Maria J Culzoni, María Eugenia Monge, Isabel Swamidoss, Dallas Mildenhall, Michael D Green, Richard Jahnke, Miguel dos Santos de Oliveira, Julia Simao, Nicholas J White, Facundo M Fernández  
paul@tropmedres.ac

Lao-Oxford-Mahosot Hospital-Wellcome Trust Research Unit, Microbiology Laboratory, Mahosot Hospital, Vientiane, Laos (PNN, PT); Centre for Tropical Medicine and Global Health, Nuffield Department of Medicine, Churchill Hospital, Oxford University, Oxford, UK (PNN, PT, NJW); Worldwide Antimalarial Resistance Network, Churchill Hospital, Oxford University, Oxford, UK (PNN, PT, NJW); London School of Hygiene & Tropical Medicine, London, UK (PNN); School of Chemistry and Biochemistry, Georgia Institute of Technology, Atlanta, GA, USA (PD, MJC, MEM, FMF); Laboratorio

de Desarrollo Analítico y Quimiometría, Cátedra de Química Analítica I, Facultad de Bioquímica y Ciencias Biológicas, Universidad Nacional del Litoral, Ciudad Universitaria, Santa Fe, Argentina (MJC); Consejo Nacional de Investigaciones Científicas y Técnicas, Buenos Aires, Argentina (MJC); Centro de Investigaciones en Bionanociencias, Consejo Nacional de Investigaciones Científicas y Técnicas, Godoy Cruz, Argentina (MEM); Centers for Disease Control and Prevention, Atlanta, GA, USA (IS, MDG); GNS Science, Lower Hutt, New Zealand (DM); Global Pharma Health Fund, Frankfurt, Germany (RJ); Inspeção Geral de Saúde, Luanda, Angola (MdSdO, JS); and Mahidol Oxford Research Unit, Faculty of Tropical Medicine, Mahidol University, Bangkok, Thailand (NJW)

- 1 Newton PN, Green MD, Mildenhall DC, et al. Poor quality vital anti-malarials in Africa—an urgent neglected public health priority. *Malaria J* 2010; **10**: 352.
- 2 Institute of Medicine. Countering the problem of falsified and substandard drugs. Washington, DC: The National Academies Press, 2013.
- 3 Attaran A, Barry D, Basheer S, et al. How to achieve international action on falsified and substandard medicines: a consensus statement. *BMJ* 2012; **345**: e7381.
- 4 Faucon B, Murphy C, Whalen J. Africa’s malaria battle: fake drug pipeline undercuts progress. *Wall Street Journal* May 29, 2013. <http://online.wsj.com/article/SB10001424127887324474004578444942841728204.html> (accessed April 18, 2014).
- 5 WHO. Falsified batches of Coartem recently circulating in Cameroon. <http://www.who.int/medicines/publications/drugalerts/drugalertindex/en/> (accessed April 18, 2014).
- 6 White NJ, Pongtavornpinyo W, Maude RJ, et al. Hyperparasitaemia and low dosing are an important source of anti-malarial drug resistance. *Malaria J* 2009; **8**: 253.
- 7 Lee KC, Ladizinski B, Federman DG. Complications associated with use of levamisole-contaminated cocaine: an emerging public health challenge. *Mayo Clin Proc* 2012; **87**: 581–86.
- 8 Cockburn R, Newton PN, Agyarko EK, Akunyili D, White NJ. The global threat of counterfeit drugs: why industry and governments must communicate the dangers. *PLoS Med* 2005; **2**: e100.
- 9 Taylor N. WHA deal breaks poor quality drugs deadlock. *Securing Industry* June 3, 2013. <http://www.securingsindustry.com/pharmaceuticals/wha-deal-breaks-poor-quality-drugs-deadlock/s40/a1746/> (accessed April 18, 2014).
- 10 WHO Regional Office for Africa. First African Medicines Regulatory Authorities Conference: Final report. Oct 31–Nov 3, 2005; Addis Ababa, Ethiopia. <http://apps.who.int/medicinedocs/en/d/j17809en/> (accessed April 18, 2014).

## Supplementary appendix

This appendix formed part of the original submission. We post it as supplied by the authors.

Supplement to: Newton PN, Taberner P, Dwivedi P, et al. Falsified medicines in Africa: all talk, no action. *Lancet Glob Health* 2014; **2**: e509–10.

## **Supplementary Material - Falsified medicines in Africa and public health – ‘No Action–Talk Only’**

Sample details are summarised in Table 1

### **Chemical Analysis**

#### **Chemicals**

Standards of mebendazole (CAS Number 31431-39-7; EC Number 250-635-4) and levamisole (CAS-No. 16595-80-5; EC-No.240-654-6, Vetranal-analytical grade) were purchased from Sigma-Aldrich Co. (St. Louis, MO, USA) in their powder form.

#### **High Performance Liquid Chromatography**

The ‘artemether-lumefantrine’ was analysed by High Performance Liquid Chromatography with Diode Array Detection (HPLC-DAD) (Agilent 1100, Agilent Technologies, Palo Alto, CA, USA). Ao-2012-1 was not analysed by HPLC-DAD due to limited sample availability. High performance liquid chromatography with diode array detection (HPLC-DAD). Two Ao-2012-2 tablets were analyzed by high performance liquid chromatography with diode array detection (Agilent 1100 Series, Agilent Technologies, Inc., Palo Alto, CA, USA) for artemether and lumefantrine. The entire tablet was weighed, pulverized, dissolved in methanol/acetic acid (9:1 v/v) and filtered through a 0.45 µm membrane. The

sample extract was injected directly into the HPLC system with UV detection wavelength set at 210 nm for artemether and lumefantrine. Component separation was achieved using a 150 x 4.6 mm C18, 5  $\mu$ m column (Supelco Analytical, Bellefonte, PA, USA) with a mobile phase consisting of 65% ACN and 35% 0.05M sodium perchlorate (pH 2.5) and flow rate of 1 mL min<sup>-1</sup>. The lower limits of detection under these conditions were equivalent to a tablet containing 2 mg of artemether and 0.05 mg of lumefantrine. Authentic tablets were also analyzed as a positive control.

### **Sample preparation for Mass Spectrometry**

For analysis of the Ao-2012-1 suspect tablet, 0.08 g of the tablet was dissolved in 10 mL of solvent (80:20 v/v solution of methanol and water with 1% acetic acid). After vortex mixing for 3 minutes followed by sonication for 30 minutes, 2  $\mu$ L of the supernatant was diluted to 300  $\mu$ L using the solvent. Mass spectrometric analysis was performed with this sample solution. Standards of mebendazole and levamisole were also prepared in methanol-water solvent. For quantitation of levamisole, a 6.57 mM stock solution of the levamisole standard was used to prepare standards ranging between 4.4  $\mu$ M and 440  $\mu$ M. For analysis of the Ao-2012-2 suspect tablet, 75.8 mg of the tablet was dissolved in 10 mL of solvent (80:20 v/v solution of methanol and water with 1% acetic acid) and protocols identical to those for Ao-2012-1 were followed.

## Mass Spectrometry

Mass spectrometry (MS) techniques were used to determine the chemical composition of sample Ao-2012-1. The MS platforms used for MS analysis were: 1) Direct analysis in real time-mass spectrometry (DART-MS), 2) DART-tandem MS (DART-MS/MS), 3) ultra-high performance liquid chromatography MS (UHPLC-MS), and 4) UHPLC-MS with travelling wave ion mobility spectrometry separation (UHPLC-TWIMS-MS) (Harris et al. 2008, Monge et al. 2013). DART-MS allows rapid analysis of solid samples under ambient conditions with minimal or no sample preparation for the determination of chemicals present in the sample. In DART with tandem MS (DART-MS/MS), detected ions are fragmented to produce product ions and the fragmentation pattern thus obtained aids in the identification and verification of the chemicals detected. Introduction of UHPLC separation prior to MS analysis, in addition to de-convoluting the mass spectrum in a second dimension by separating the chemicals present in a mixture solution, provides a secondary parameter (retention time), for compound identity verification. Further introduction of TWIMS separations in the UHPLC-MS platform provides an additional analytical parameter (drift time) for compound identity verification, in addition to separating the chemicals in the third dimension prior to analysis by mass spectrometry. Thus, utilizing these platforms a chemical can be identified and its identity validated using five parameters specific to the chemical of interest. These parameters are 1) mass-to-charge ratio of the analyte ion along with its specific adduct or cluster ions, 2) isotopic distribution matching, 3) fragmentation pattern, 4) retention time, and 5) drift time.

For DART-MS and DART-MS/MS analysis, a commercial DART-100 ion source (IonSense, Saugus, MA, USA) was coupled in-line through a VAPUR interface (IonSense, Saugus, MA, USA) with a Bruker micrOTOF-Q I mass spectrometer (Bremen, Germany). Detailed description of the DART-100 ion source is available elsewhere (Cody et al. 2005, Cody et al. 2005). The DART working gas (high purity He, 99.995% Airgas, Atlanta, GA) was supplied to the ion source at a flow rate of 1 L min<sup>-1</sup> and was heated to 250 °C. The DART ion source and the mass spectrometer voltage settings were optimized for maximum ion transmission in the m/z range of 50-1200. The mass spectrometer was mass calibrated using a 10 µM methanol solution of PEG 400, PEG 600, and PEG 1000 calibration standards. The mass spectrometer provided a mass resolution of ~12,000 at m/z 393.2095 and ~9,000 at m/z 151.0964, and a typical mass accuracy of 2-5 ppm was obtained for acetaminophen as test compound. Experiments were performed in both positive and negative ion detection mode. For analysis of tablets, the coating was scratched with a razor blade, a few tablet particles were obtained by scratching the inside and outside surfaces of the tablet, the particles were placed on a Kimwipe, and deposited on the tip of a glass capillary by rubbing it against the Kimwipe. The capillary tip with the deposited sample was then introduced in front of the plasma plume exiting the DART source for sample ionization and subsequent detection by mass spectrometry. Powders of chemical standards were deposited on the capillary tip and analysed under identical experimental and instrumental conditions as those used for tablet analysis. The Bruker Daltonics DataAnalysis Version 4.0 software package was used for processing of all acquired data. Presence and identity of active pharmaceutical ingredients (APIs) and

excipients in the sample tablet was established by matching  $m/z$  values measured by the mass spectrometer with calculated exact  $m/z$  values, and values measured for the API standards, together with the isotopic abundances, and adduct, or fragment ions.

For UHPLC-MS and UHPLC-TWIMS-MS analysis a Waters ACQUITY Ultra Performance LC (Waters Corporation, Manchester, UK) system, coupled to a Synapt G2 High Definition Mass Spectrometry system (Waters Corporation, Manchester, UK), which is a hybrid quadrupole-ion mobility-orthogonal acceleration time-of-flight instrument (Benton et al. 2012, Giles et al. 2004, Pringle et al. 2007) was used. The UHPLC system was fitted with a Waters ACQUITY UHPLC BEH  $C_{18}$  column ( $1.0 \times 100$  mm,  $1.7 \mu\text{m}$  particle size). The traveling wave ion mobility spectrometry (TWIMS) separation mode of the Synapt system was activated and optimized for UHPLC-TWIMS-MS analysis. All analyses were performed in the positive ion detection mode of the instrument. The mass spectrometer was calibrated across the 50-1200  $m/z$  range using a 0.5 mM sodium formate solution prepared in 90:10 2-propanol:water v/v. Data were mass corrected during acquisition using a leucine enkephalin reference spray (LockSpray) infused at  $2 \mu\text{L min}^{-1}$ . Data acquisition and processing was carried out using Mass Lynx v4.1 and Drift Scope v2.1 (Waters Corp.). Chromatographic separation was achieved using acetonitrile (ACN) and water with 1% acetic acid as mobile phase solvents and gradient elution with 10% ACN to 100% ACN in 4 minutes. During the total run time of 6 minutes, mobile phase composition was 100% ACN between minute 4 and 5 and was reverted back to 10% ACN at 5.4 minutes. The mobile phase flow rate was  $0.3 \text{ mL min}^{-1}$ , the column temperature was



45°C, the autosampler tray temperature was set to 5°C, and the injection volume was 5 µL.

### **X-ray diffraction analysis**

X-ray powder diffraction (XRD) analysis based on diffraction peak angles and corresponding intensities can be employed to identify bulk unknown excipients. Experimentally-obtained XRD scans can be searched on powder diffraction files (PDF) databases to identify the unknowns in the sample. The powder diffraction files database is a collection of d-I data—the d-spacing (d) determined from the angle of diffraction and the intensity (I), experimentally measured for a phase-pure material. These data provide a “fingerprint” of the compound because the d-spacings are fixed by the geometry of the crystal and the intensities are dependent on the elements and their arrangement in the crystal structure. Thus, the d-I data can be used for identification of unknown materials by locating matching d-I data in the PDF with the d-Is obtained from the unknown. Experiments were run using a PANalytical XRD – Alpha-1 instrument with X’pert data acquisition program. The instrument emits  $K\alpha_1$  radiation with a Cu source. Experimental parameters included a scan time of 40 minutes with step size of 0.02 degrees. The beam width was restricted to 15 mm by use of a mask. Soller slit packs of 0.04 rad were used in the pre-diffraction and post-diffraction optics with  $\frac{1}{2}$  anti-scatter slit and 5 mm receiving slit. The acquired scan was analyzed using PDF-4+ and High score plus software supported by the d-I database.

### **MS pigment analysis**

UHPLC-MS was also used to investigate the presence of pigments in sample Ao-2012-2. For that purpose, 0.05 g of pulverized sample was dissolved in 2 mL of tetrahydrofuran. Then, the solution was sonicated for 30 minutes, and centrifuged at 13,000 rpm for 20 minutes. UHPLC-MS analysis was performed in the negative ion mode. Chromatographic separation was achieved in 10 minutes using ACN and water with 1% acetic acid as mobile phase solvents and gradient elution with 5% ACN to 95% ACN in 8 minutes, which was reverted back to 5% ACN at 9 minutes. The mobile phase flow rate was  $0.3 \text{ mL min}^{-1}$ , the column temperature was  $50^{\circ}\text{C}$ , the autosampler tray temperature was set to  $5^{\circ}\text{C}$ , and the injection volume was  $10 \text{ }\mu\text{L}$ .

## **IRMS**

Isotopic mass measurements were made using a Finnigan MAT253 IRMS mass spectrometer with Kiel carbonate preparation device. Values were calibrated using NBS-19 and NBS-18, and internal precision met or exceeded  $0.08\text{‰}$  (1 sigma or 1 standard deviation of replicate analyses of NBS-19 or of other in house standards).

## **NMR analysis**

NMR experiments were performed at a temperature of 298 K on a Bruker-Biospin Avance II 500 NMR spectrometer, operated at a  $^1\text{H}$  frequency of 500 MHz. The instrument was equipped with a 5 mm  $^1\text{H}/\text{X}$ -broadband probe with gradient in the z-direction. Acquisition parameters for the 1D  $^1\text{H}$  NMR experiments comprised  $^1\text{H}$  excitation with a 30 degree pulse followed by an acquisition of 65536 data points during a time of 3.17 s; and followed by a recycle delay of 1 s. A total of 16 scans were accumulated. Data were referenced with respect to the solvent peak of the

deuterated dimethyl sulfoxide (DMSO) at 2.5 ppm. The parameters for 2D DOSY  $^1\text{H}$  NMR experiments were as follows: LED pulse sequence with bipolar gradients,  $\Delta=50$  ms diffusion time,  $\delta=2.2$  ms gradient duration; 2s repetition delay, and 16 averages. Diffusion was encoded using gradient pulses with a sinusoidal shape with 16 gradient steps ranging from 0.7 to 32 Gauss  $\text{cm}^{-1}$ . All NMR data were processed using TOPSPIN software (Bruker). Samples were prepared by dissolving a mass of powdered tablets equivalent to 5 mg of analyte in 0.7 mL of deuterated DMSO, followed by sonication for 15 minutes, and centrifugation (3 min,  $13,000 \times g$ ). The supernatant was poured into a 5-mm NMR tube for analysis. Individual standards of artemether, lumefantrine, mebendazole, and levamisole were prepared in DMSO providing final concentrations of 5 mg  $\text{mL}^{-1}$ .

### **Botanical Assays**

Pollen processing of eight tablets from suspect sample Ao-2012-2 and eight from authentic sample G-NOV-62 were identical in each case with weighing, crushing, hot water wash, acetolysis, hot 10% HCl, acetone wash, filtering through a 6  $\mu\text{m}$  filter and mounting in unstained glycerine jelly on two slides under long coverslips (the total amount of residue remaining) (Newton *et al.* 2008). All slides were examined using an Axioplan 2 imaging microscope under a  $10 \times$  eyepiece, a  $\times 1.25$  Optovar and objectives at  $\times 10$ , 20 and 100. Spores and pollen were identified under a total magnification of between 500 and 1000 times. Slides are stored in the palynological slide collection of GNS Science. A slide with glycerine jelly was exposed in the laboratory as a check for possible laboratory contamination by pollen (the laboratory has negative air pressure to prevent this happening). No pollen was found.

### **Packaging Analysis**

Packaging analysis was conducted on Ao-2012-1 and Ao-2012-2 using the hand held portable Counterfeit Detection Device #3 (CD-3) (Ranieri *et al.* submitted) (Figures 1 & 2, Table 1). Analysis was performed in comparison to a genuine product and the differences in appearance and inner and outer packaging documented. The CD-3 device is used to screen pharmaceutical products using an alternate light source with multiple wavelengths in the visible (350 - 700 nm) and non-visible (>700 nm) electromagnetic spectrum. Images of the different inks (pigments/dyes) on the package and tablets of the falsified medicines versus the authentic products were captured in the CD-3 device. The genuine comparator for Ao-2012-1 was G-JJ-68: Vermox 500 mg, manufactured by Janssen-Cilag SpA, Latina Italy, batch number CIL8J00 and expiry date 09/2015; and for Ao-2012-2 was G-NOV-65: Coartem 20/120, manufactured by Novartis Pharmaceuticals Corporation, New York, USA, batch number F2851 and expiry date 06/2014. Analysis conducted under UV-Vis and infrared light revealed significant differences between the suspect samples and the genuine comparators.

### **Reporting**

We have used the distinction between falsified (or counterfeit or spurious medicines; *i.e.* ‘deliberately and fraudulently mislabeled with respect to identity and/or source’) and substandard medicines (*i.e.* ‘genuine medicines produced by manufacturers authorized....which do not meet quality specifications set for them by national standards’) (World Health Organization. 2008). To avoid any intellectual property

connotations the term falsified is used here instead of counterfeit (Newton *et al.* 2011, Attaran *et al.* 2012).

The results are presented using the MEDQUARG guidelines (Newton *et al.* 2009), and were reported to the Angolan Inspeção Geral de Saúde, WHO Rapid Response (World Health Organization. 2013a,b,c), the manufacturers of the genuine products, United Nations Office on Drugs and Crime, the World Customs Organization and the Uppsala Monitoring Centre.

## **Results**

### **Sample Ao-2012-2**

#### *Active Pharmaceutical Analysis*

No detectable levels of artemether or lumefantrine were observed by HPLC-DAD. MS and XRD methods described above were used to determine the chemical composition of the sample tablet Ao-2012-2. Figure 3 show the DART-MS analysis of a Coartem 20/120 sample, tablet # FE 24, manufactured by Novartis Pharmaceuticals Corporation, that contained the active ingredients artemether and lumefantrine, illustrating the theoretical  $m/z$  values, and isotopic pattern of artemether and lumefantrine response ion peaks for artemether and lumefantrine, and the DART-MS analysis of sample Ao-2012-2, zoomed into the mass spectral

region of the expected artemether and lumefantrine response peaks. Ionization of artemether by DART usually generates an ammonium adduct of the artemether molecule of type  $[M+NH_4]^+$  with an exact mass of 316.2118 Da. The response peak for the genuine tablet was detected at  $m/z$  value of 316.2192 and the isotopic distribution matched with that theoretically expected. DART ionization of lumefantrine usually generates a protonated ion of type  $[M+H]^+$  with an exact mass of 528.1622 with a chlorine signature clearly evident in the isotopic distribution. The lumefantrine peak at  $m/z$  value of 528.1731 and the lumefantrine peak pattern as shown in Figure 3 were easily detected when the genuine tablet FE-24 was analysed. However, neither peak nor pattern was detected, even at various sample desorption temperatures (100-450 °C) when the sample tablet Ao-2012-2 was analysed. The experiment clearly demonstrated the absence of artemether and lumefantrine in the sample tablet Ao-2012-2.

For further confirmation of the absence of the expected APIs in the sample Ao-2012-2, the tablet was subjected to analysis by UHPLC-MS and UHPLC-TWIMS-MS. A tablet solution, when analysed by the above methods, did not show any signature of the expected APIs, supporting the DART-MS analysis results.

#### *Excipient analysis*

Positive and negative mode DART-MS and DART-MS/MS analysis of the suspect tablet Ao-2012-2 suggested the presence of polysaccharides as excipients in the

tablet. As demonstrated in Figure 4 positive mode analysis suggested the presence of a disaccharide in the sample. In the negative mode analysis of the sample, a series of peaks were detected, with a difference of 162.05 Da corresponding to a dehydrated hexose molecule ( $C_6H_{12}O_6 - H_2O$ ) with the largest detected saccharide at  $m/z$  925.2 corresponding to a pentasaccharide. This suggests that either a mixture of polysaccharides is present in the tablet or the polysaccharide is undergoing fragmentation between the ion source and the mass spectrometer inlet. Moreover, neutral loss of a phosphoric acid fragment when the tetrasaccharide and the pentasaccharide were subjected to collision induced dissociation (CID) suggests the presence of phosphates in the sample. Detection of only the disaccharide, in positive ion mode may be caused by fragmentation of the pentasaccharide prior to MS detection, possibly in the ionization region, to produce the disaccharide. Nonetheless, both positive and negative mode DART-MS and DART-MS/MS analysis suggest the presence of saccharides in the tablet. Furthermore, the mass peak at  $m/z$  283.1794 seen in positive mode analyses was tentatively identified as the  $[(C_2H_4O)_6 + H_2O + H]^+$  polyethylene glycol (PEG) ion and the fragmentation pattern (shown in Figure 4 B) suggests the presence of PEG and its fragments at  $m/z$  values of 267.1522, 239.1556, and 149.0249.

Figure 5 indicates the XRD identification of one of the excipients present in the sample as brushite, a pale yellow mineral of chemical formula  $CaHPO_4 \cdot 2H_2O$ . The sample produced the peaks shown in red and the blue lines represent the peaks expected for brushite based on that reported in the PDF database. Detection of

brushite can also explain the phosphoric acid loss in the polysaccharides DART-MS and DART-MS/MS experiments.

### *Pigment analysis*

UHPLC-MS sample analysis revealed the presence of pigment yellow 3, pigment yellow 81 and pigment yellow 151 in Ao-2012-2. Figures 6 A-C illustrate the extracted ion chromatograms for the  $[M-H]^-$  ions at theoretical  $m/z$  380.0995 for pigment yellow 151 ( $C_{18}H_{15}N_5O_5$ ),  $m/z$  393.0157 for pigment yellow 3 ( $C_{16}H_{12}Cl_2N_4O_4$ ) and  $m/z$  751.1161 for pigment yellow 81 ( $C_{36}H_{32}Cl_4N_6O_4$ ), which exhibited retention times of 4.18 min, 6.99 min and 8.10 min, respectively. For each pigment, elemental formulae were generated based on the expected mass accuracy and experimental isotopic pattern. Mass spectra for each target compounds are displayed in Figure 6 D-F, with monoisotopic peaks at  $m/z$  380.1034 ( $\Delta m=3.9$  mDa) for pigment yellow 151,  $m/z$  393.0125 ( $\Delta m=3.2$  mDa) for pigment 3, and  $m/z$  751.1196 Da ( $\Delta m=3.5$  mDa) for pigment 81, confirming the identity of these compounds.

### **Botanical Assays**

The authentic sample G-NOV-62 contained fine cellular and amorphous organic material, including plant fragments, black chips and rounded crystals of starch. A relatively large number of fungal spores with very rare pollen, including *Pinus*, Poaceae and *Casuarina* were found. A common fungal spore had a thick dark cell



wall, 3-4 pores and diameter 20-50  $\mu\text{m}$ . Tablets from Ao-2012-2 contained some *Pinus* and *Coprosma* pollen. Further analysis of photographs of the fungal spores suggests that sample Ao-2012-2 contains *Epicoccum nigrum* spores. This is a fungus associated with dead herbaceous stems and grasses but is of global distribution. The pollen and spore analysis therefore did not give any firm clues as to the origin of the raw ingredients or place of manufacture of Ao-2012-2. However, brushite is associated with environments with only sparse vegetation present and is relatively common in India and is also used extensively in Chinese herbal medicines and as cement in orthopaedics (Tamimi *et al.* 2012).

## **Packaging**

The packaging of Ao-2012-2 differed from that of a genuine sample (Table 1 A, Figure 1), strongly suggesting that the sample was falsified, consistent with chemical analysis conclusions. The details of all errors are not disclosed in this report to avoid assistance to criminals. The stapling of the sample card, incorrect manufacture and expiry date interval stamps, much thinner card and lower card weight, the use of ‘-‘ in ‘Anti-malarial agent’ differ from those on the genuine. In addition, the tablets of Ao-2012-2 were pitted, in contrast to the smooth surface of the genuine tablets. When examined and compared against the front of the blister with CD-3 using UV-Visible light, Ao-2012-2 had a brighter red colour for the dosage text, a greener blister colour and a lighter AMFm logo colour. Also under UV-Visible light, the background colour of the reverse of the blister was yellow for the genuine sample but greener for Ao-

2012-2. The colour of the falsified tablets was greener than the tablets from the genuine sample (Figures 7 & 8).

### **Sample Ao-2012-1**

#### *Active Pharmaceutical Ingredient Analysis*

DART-MS and DART-MS/MS analysis of the levamisole standard and the suspect tablet are shown in Figure 9 B-E. Two major response ions at  $m/z$  values of 409.1484 and 205.0849 were observed when sample Ao-2012-1 was analysed by DART-MS in positive ion mode. Due to low relative intensity of the peak at  $m/z$  409.1484 with respect to the peak at  $m/z$  205.0849, only the latter is displayed in the figure. The tablet was supposed to contain mebendazole as the API, and should have produced a protonated ion peak at  $m/z$  296.1029. When the standard of mebendazole was analysed, a protonated ion of mebendazole of type  $[M+H]^+$  at  $m/z$  296.1124 was detected, where M represents the neutral molecule. Peaks at  $m/z$  values corresponding to different adduct, fragments, and clusters of mebendazole were also searched for, but not found in the mass spectrum of sample Ao-2012-1. Identification of the chemical present in the suspect tablet in place of mebendazole was then carried out. Collision induced dissociation (CID) of the ion at  $m/z$  409.1484 generated a product ion at  $m/z$  205.0842; CID of the ion at  $m/z$  205.08 produced a major product ion at  $m/z$  178.0729 (Figure 9 C). From these results it was tentatively inferred that the ion at  $m/z$  409.1484 was a dimer ion,  $[2M+H]^+$ , of

an analyte that produced a monomer at  $m/z$  205.0849. Search within the NIST (National Institute of Standards and Technology) database for a protonated monomer  $[M+H]^+$  ion with  $m/z$  205 that produces a product ion at  $m/z$  178 suggested the tentative identity of the response peak to be levamisole (Figure 9 A). The exact mass of the  $[M+H]^+$  ion of levamisole is 205.0799 Da. For confirmation of the tentatively identified compound, a levamisole standard was purchased and subjected to DART-MS and DART-MS/MS analysis. Analysis of the levamisole standard produced a response ion peak at  $m/z$  value of 205.0862 which when subjected to CID generated a major product ion at  $m/z$  178.0729 tentatively identified as  $[M-HCN+H]^+$ . The experiment thus suggested that the suspect tablet does not contain mebendazole, but it contains levamisole instead.

To further confirm the identity of the chemical present in the tablet, the sample tablet and the mebendazole and levamisole standards were analysed by UHPLC-MS and UHPLC-TWIMS-MS. Figure 10 shows the results of the UHPLC-MS analysis of the tablet and the standards. Chromatographic retention time for the mebendazole standard was 2.04 minutes. The extracted mass spectrum from this chromatographic peak showed signals corresponding to the protonated ion and the fragment ion of mebendazole at  $m/z$  296.1014 and  $m/z$  264.0757, respectively. The sample tablet did not show any chromatographic peak at ~2 minutes, however, a doublet peak in the retention time range of 1.1-1.37 minutes was detected. The mass spectrum extracted from the doublet chromatographic peak showed the presence of signals at  $m/z$  205.0771 and  $m/z$  178.0708. Subsequent analysis of a

levamisole standard also produced a chromatographic doublet peak in the retention time range of 1.1 -1.37 minutes, similar in shape to that observed for Ao-2012-1. The extracted mass spectrum from this chromatographic peak showed the presence of signals at  $m/z$  205.0771 and  $m/z$  178.0708 corresponding to the protonated precursor and product ions of levamisole as discussed earlier. To add to the identification confidence, ion mobility separation (IMS) (Kanu *et al.* 2008, Eiceman & Karpass 1993) that separates ions based on their size-to-charge ratio ( $\Omega/z$ ) instead of the mass-to-charge ratio ( $m/z$ ) was also performed. Ions of same  $m/z$  can be separated by IMS if they have different size-to-charge ratios, such as in the case of isobars that are impossible to separate by MS alone. Under identical experimental and instrumental conditions, the parameter termed as “drift time” is specific for a chemical and is used as a chemical characterization parameter. Figure 11 shows results of the UHPLC-TWIMS-MS analysis. Both the suspect sample and the levamisole standard produced peaks at  $m/z$  205.0771 and  $m/z$  178.0708, respectively; with a retention time of 1.1-1.37 min and a drift time of 2.48 ms. The mobility peak also was a doublet peak supporting the inference that structural isomers of levamisole are present in the sample as well as in the standard. These experiments thus confirmed the absence of mebendazole in the tablet and the unexpected presence of levamisole.

#### *Quantitation of levamisole in Ao-2012-1*

For quantitation of levamisole, a 6.57 mM stock solution and standards ranging between 4.4  $\mu$ M and 440  $\mu$ M were prepared. Standard solutions and that of the sample tablet were analysed by UHPLC-MS/MS in duplicate. A calibration curve was established using the levamisole chromatographic peak area then used to calculate the concentration of levamisole present in the tablet (Figure 12). Based on the weight of tablet and the dilution factors used, the sample Ao-2012-1 contained 0.36 grams of levamisole per gram of tablet weight. With a tablet weight of ~750 mg this yields 270 mg levamisole/tablet.

#### *Excipient MS analysis*

Negative mode DART-MS analysis of the suspect tablet suggested the presence of a disaccharide (such as lactose) in the tablet. As illustrated in Figure 13 A-B, ions at  $m/z$  values of 359.0739, 323.0956, 283.2637, 255.2328 and 150.0565 were detected. The ion at  $m/z$  359.0739 was tentatively assigned to a disaccharide (exact mass 342.1157 Da) observed as the deprotonated water adduct,  $[M+H_2O-H]^-$ . Negative ions formed after the neutral loss of two water molecules from this adduct result in the peak at  $m/z$  323.0956. Further fragmentation of the disaccharide generates the product ion of type  $[M-C_5H_8O_5-H_2O-H]^-$  at  $m/z$  194.0442. Fragmentation and isotopic distribution patterns of the ion at  $m/z$  359.07 supported the tentative identification of this excipient as a disaccharide, such as lactose. Furthermore, the signal at  $m/z$  283.2637 was tentatively identified as stearic acid, forming an ion of type  $[M-H]^-$  with an exact mass of 283.2631. The product ion detected at  $m/z$

255.2328 was assigned to an ion of type  $[M-C_2H_4-H]^-$  generated with the loss of  $C_2H_4$  from the aliphatic chain of the stearic acid molecule (M) with an exact mass of 255.2319.

#### *XRD analysis*

Figure 13 C demonstrates the XRD identification of one of the excipients present in the sample as calcite ( $CaCO_3$ ). The sample produced the peaks shown in red and the blue lines represent the diffraction pattern expected for calcite based on that reported in the PDF database.

#### **Packaging analysis**

Errors in language on the packet and the leaflet strongly suggested that the sample was falsified, corroborating chemical analysis results (Table 1 B, Figure 2). Language errors were common, suggesting that the forger may have had some knowledge of English but little of French and Spanish. The details of all errors are not disclosed in this report to avoid assistance to criminals. The batch numbers on the blister and packet were invalid. However, the packet was stamped with a valid Nigerian National Medicines Regulatory Agency (NAFDAC) registration number. Interestingly, the genuine leaflet had one English error in the pregnancy and lactation section ‘Mebendazolehas....’, that was also found on the leaflet of the falsified sample.

UV-Visible and infrared images of the falsified and genuine packaging readily demonstrated significant differences between them. On the suspect sample outer packaging the dosage information text had a brighter red colour relative to that observed for the genuine sample. The shaded area on the front of the outer packet of the genuine product was darker in colour than that observed on the suspect sample packet. In addition, differences in the texture and printing of the packet as well as in the stamped expiry date and batch information between the suspect and the genuine samples were evident (Figure 14). Unlike that observed for the genuine sample, the letters printed on the falsified inner packaging were not apparent under infrared light.

## References

1. Monge ME, Harris GA, Dwivedi P, Fernandez FM. Mass Spectrometry: Recent Advances in Direct Open Air Surface Sampling/Ionization. *Chem Rev* 2013; **113**: 2269-2308 .
2. Harris GA, Nyadong L, Fernandez FM. Recent developments in ambient ionization techniques for analytical mass spectrometry. *Analyst* 2008; **133**: 1297-301. PMID:2008:1135082.
3. Cody RB, Laramée JA, inventors; JEOL USA, assignee. Atmospheric Pressure Ion Source. USA patent 6949741. 2005.

4. Cody RB, Laramée JA, Durst HD. Versatile new ion source for the analysis of materials in open air under ambient conditions. *Anal Chem* 2005, **77**: 2297-302. PMID:15828760.
5. Benton CM, Lim CK, Moniz C, Jones DJL. Travelling wave ion mobility mass spectrometry of 5-aminolaevulinic acid, porphobilinogen and porphyrins. *Rapid Comm Mass Spect* 2012, **26**: 480-6. PMID:WOS:000299739700010.
6. Giles K, Pringle SD, Worthington KR, Little D, Wildgoose JL, Bateman RH. Applications of a travelling wave-based radio-frequencyonly stacked ring ion guide. *Rapid Comm Mass Spect* 2004; **18**: 2401-14. PMID:ISI:000224499400006.
7. Pringle SD, Giles K, Wildgoose JL, Williams JP, Slade SE, Thalassinou K, Bateman RH, Bowers MT, Scrivens JH. An investigation of the mobility separation of some peptide and protein ions using a new hybrid quadrupole/travelling wave IMS/oa-ToF instrument. *Int J Mass Spect* 2007; **261**: 1-12.
8. Newton PN, Fernández FM, Plançon A et al. A Collaborative Epidemiological Investigation into the Criminal Fake Artesunate Trade in South East Asia. *PLoS Med* 2008; **5**: e32.
9. Ranieri N, Tabernero P, Green MD et al. (submitted) Evaluation of a new hand held device for the detection of counterfeit artesunate by visual fluorescence comparison. *AJTMH*



10. World Health Organization. Executive Board 124th session provisional agenda item 4.11. Counterfeit medical products. EB124/14. 2008. Available: [http://apps.who.int/gb/ebwha/pdf\\_files/EB124/B124\\_14-en.pdf](http://apps.who.int/gb/ebwha/pdf_files/EB124/B124_14-en.pdf). With corrigendum: [http://apps.who.int/gb/ebwha/pdf\\_files/EB124/B124\\_14Corr1-en.pdf](http://apps.who.int/gb/ebwha/pdf_files/EB124/B124_14Corr1-en.pdf). Accessed 18th January 2014.
11. Newton PN, Amin A, Bird C et al. The primacy of public health considerations in defining poor quality medicines. *PLoS Med* 2011; **8**: e1001139.
12. Attaran A, Barry D, Basheer S et al. How to Achieve International Action on Falsified and Substandard Medicines: A Consensus Statement. *BMJ* 2012; **345**: e7381.
12. Newton PN, Lee SJ, Goodman C et al. Guidelines for field surveys of the quality of medicines: a proposal. *PLoS Med* 2009; **6**: e1000052.
13. World Health Organization. WHO project for the surveillance and monitoring of SSFFC medical products. *WHO Drug Info* 2013; **27**: 97–100.
14. World Health Organization. Falsified batches of Coartem recently circulating in Western and Central Africa. QSM/MC/IEA.127. 3 May 2013. Information Exchange System. Alert No. 127. WHO, Geneva. Available at: <http://www.who.int/medicines/publications/drugalerts/drugalertindex/en/>. Accessed 18th April 2014.

15. World Health Organization. Falsified batches of Coartem recently circulating in Cameroon. RHT/SAV/MD/IEA.130.127. 8 November 2013. Information Exchange System. Alert No. 130. WHO, Geneva. Available at: <http://www.who.int/medicines/publications/drugalerts/drugalertindex/en/>. Accessed 18th April 2014.
16. Tamimi F, Sheikh Z, Barralet J. Dicalcium phosphate cements: brushite and monetite. *Acta Biomater* 2012, **8**: 474-87.
17. Kanu AB, Dwivedi P, Tam M, Matz L, Hill HH, Jr. Ion mobility-mass spectrometry. *J Mass Spectrom* 2008, **43**: 1-22. PMCID:18200615.
18. Eiceman GA, Karpass Z. *Ion Mobility Spectrometry*. CRC Press; 1993.

**Table 1A. Distinguishing features of falsified artemether-lumefantrine labelled as made by Novartis.** Details of some errors have been omitted to avoid assisting those producing the falsified product. These details may be requested from the corresponding author.

Variable	Genuine	Falsified
	<b>G-NOV-65</b>	<b>Ao-2012-2</b>
<b>Packet</b>		
Stated manufacturer	‘Manufactured by: Novartis Pharmaceuticals Corporation, Suffern, New York, USA for Novartis Pharma AG, Basle, Switzerland, under licence from the PRC 5002835’	‘Manufactured by: Novartis Pharmaceuticals Corporation, Suffern, New York, USA for Novartis Pharma AG, Basle, Switzerland, under licence from the PRC 5002835’
No. tablets	24	24
Tablet text	CG N   C	CG N   C
Tablet appearance	Surface pitted without clear ‘lines’	Surface smooth with clear ‘lines’
Tablet diameter/thickness/mm	9.10/3.10 *	9.50/3.50
Tablet colour RGB % above ‘C’	R 130 G 127 B 40	R 125 G 125 B 46
Folded blister enclosure	Folded and glued	Folded and stapled
Logos	ACTm Mosquito and shadow	ACTm Mosquito and shadow
Batch:	F2851	F2261
Mfd:	07 2012	01 2012
Exp:	06 2014	01 2014
	Difference between Mfd and Exp of 23 months	Difference between Mfd and Exp of 24 months
Packet card thickness	0.45 mm	0.25 mm
Packet length and width	11.8 cm x 14.9 cm	11.8 cm x 14.9 cm
Packet weight (without blister & tablets)/g	8.48	5.94
Text differences	Anti malarial agent	Anti-malarial agent
<b>Blister</b>		
Text	Coartem ® (artemether/lumefantrine) 20 mg/ 120 mg Tablets logo NOVARTIS	Coartem ® (artemether/lumefantrine) 20 mg/ 120 mg Tablets logo NOVARTIS

	5002092	5002092
Embossed	F 2851 06 2014	1- 1901 01 2014
<b>Tablet chemical analysis</b>		
DART MS, ESI-MS, UHPLC-MS and ESI-UHPLC-TWIMS-MS	Artemether and lumefantrine detected	Artemether and lumefantrine not detected
DART-MS, DART-MS/MS	Artemether and lumefantrine detected	Polysaccharides and polyethylene glycol
HPLC-UV	Artemether and lumefantrine detected	Artemether and lumefantrine not detected
XRD	N/A	Brushite, $\text{CaHPO}_4 \cdot 2\text{H}_2\text{O}$
Raman	Signature very similar to genuine	Signature very different from that of genuine
NMR	Artemether and lumefantrine detected.	Artemether and lumefantrine not detected. Signature very different from that of genuine
<b>Tablet pollen and spore analysis</b>	<b>G-NOV-62</b>	<b>Ao-2012-2</b>
Acetolysis	Solution turned <b>black</b> after 5 minutes indicating the presence of corn starch	Solution turned <b>yellow</b> after 5 minutes and remained yellow throughout processing
	Fine cellular and amorphous organic material, including plant fragments and black chips. Rounded crystals of starch present. A relatively large number of fungal spores with very rare pollen, including <i>Pinus</i> , Poaceae and <i>Casuarina</i> . A common fungal spore had a thick dark cell wall and 3-4 pores and diameter 20-50 $\mu\text{m}$ . The fungal spores were identified from photographs as <i>Alternaria</i> sp. and <i>Monodictys</i> sp.	<i>Pinus</i> , <i>Coprosma</i> pollen and <i>Epicoccum nigrum</i> spores

Weight and thickness specification ranges for Coartem are 0.228-0.252 g and 3.0-3.4 mm, respectively (Novartis pers. comm.)

**Table 1B. Features of falsified mebendazole labelled as ‘Vermox® 500mg’ made by ‘Janssen-Cilag’.** Details of some errors removed to avoid assisting those producing the falsified product. These details may be requested from the corresponding author.

Variable	Genuine	Falsified
Packet	G-JJ-68	Ao-2012-1
Stated manufacturer	‘JANSSEN-CILAG’	‘JANSSEN-CILAG’
	‘Manufactured by: JANSSEN-CILAG SpA. – V.C. JANSSEN - Borgo S. Michele – 04010 Latina – Italy for Janssen Pharmaceutica N.V., Turnhoutseweg 30, B-2340 Beerse, Belgium’	‘Manufactured by: JANSSEN-CILAG SpA. – V.C. JANSSEN - Borgo S. Michele – 04010 Latina – Italy for Janssen Pharmaceutica N.V., Turnhoutseweg 30, B-2340 Beerse, Belgium’
Other text	mebendazol 500 mg para un comprimido  1 tableta oral	mebendazol 500 mg para un comprimido  1 tableta oral
Colour of inside surface of packet	Creamy white	<b>Matt white</b>
Text language	French, English, Spanish	French, English, Spanish
Batch no :	CIL8J00	9CL2400
Mfg. date :	10-2012	09-2011
Expiry :	09-2015	08-2014
<b>Other Codes</b>	NAFDAC REG. No. 04-1682	NAFDAC REG. No. 04-1682
	NG 963564 116	NG 963564 116
<b>Bar Codes</b>	Two bar codes on two side tabs	Two bar codes on two side tabs
<b>Blister</b>		
No. of tablets	1	1
Tablet colour	White	White
Tablet weight/mg		~750
BN	CIL8J00	AII 0800
Mfg/Exp:	10-2012/09-2015	09-2010 / 08-2013
BN and Mfg/Exp:	embossed	Embossed
Logo		<b>Stylised ‘horse’ logo design on blister and packet not the same</b>
<b>Leaflet</b>		
Leaflet weight/g	5.94	<b>6.51</b>
<b>Tablet chemistry</b>		
DART MS, UHPLC-MS	Mebendazole	<b>No mebendazole detected. Levamisole</b>

and UHPLC-TWIMS-MS		detected
ESI-UHPLC-MS	Mebendazole	Levamisole concentration = 0.36 grams of levamisole /gram of tablet weight. With a tablet weight of ~ 750mg this gives 270 mg levamisole /tablet
Excipient DART-MS	N/A	carbohydrates & stearic acid
Excipient X-ray powder diffraction (XRD)	N/A	calcite
Calcite IRMS	N/A	hydrothermal or medical in origin

## Figures

**Figure 1.** Scanned pictures of samples: top) falsified blister; Ao-2012-2, bottom) genuine blister.





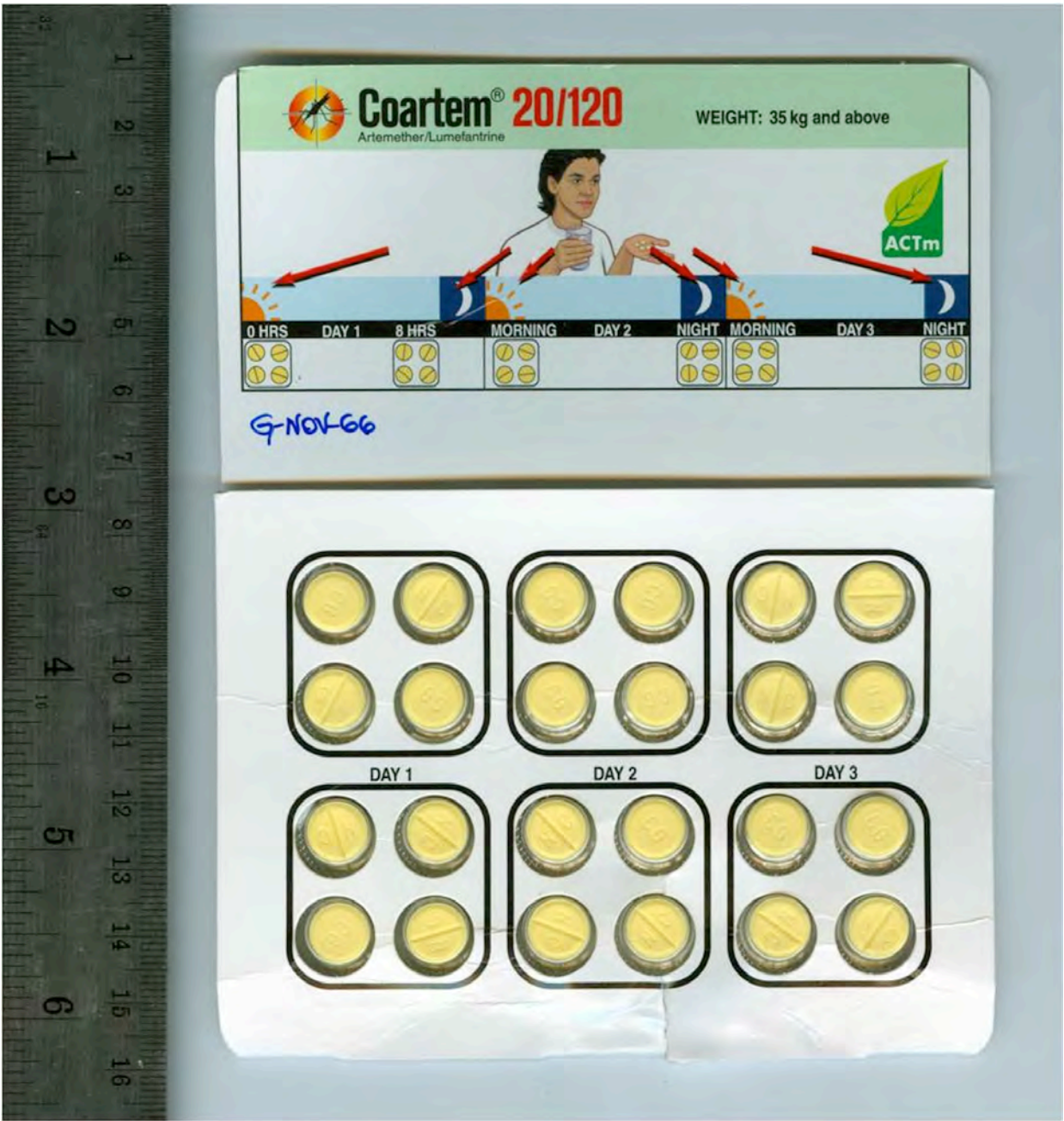




**Figure 2.** Scanned pictures of samples: top) falsified packet; Ao-2012-1, bottom) genuine packet.





**Figure 3.** Positive mode DART-MS spectra of a genuine Coartem 20/120 (sample # FE-24) manufactured by Novartis pharmaceuticals showing the detection of A) artemether as its  $[M + \text{NH}_4]^+$  ion; B) theoretical  $m/z$  value and isotopic distribution of artemether; C) lumefantrine as its  $[M + \text{H}]^+$  ion; D) theoretical  $m/z$  values and isotopic distribution of lumefantrine; E) full mass spectrum of genuine sample (FE-24) in the  $m/z$  range of 290-550 showing the presence of both artemether and lumefantrine peaks; and F) full mass spectrum of sample # Ao-2012-2 in the  $m/z$  range of 290-550 showing the absence of artemether and lumefantrine signals.

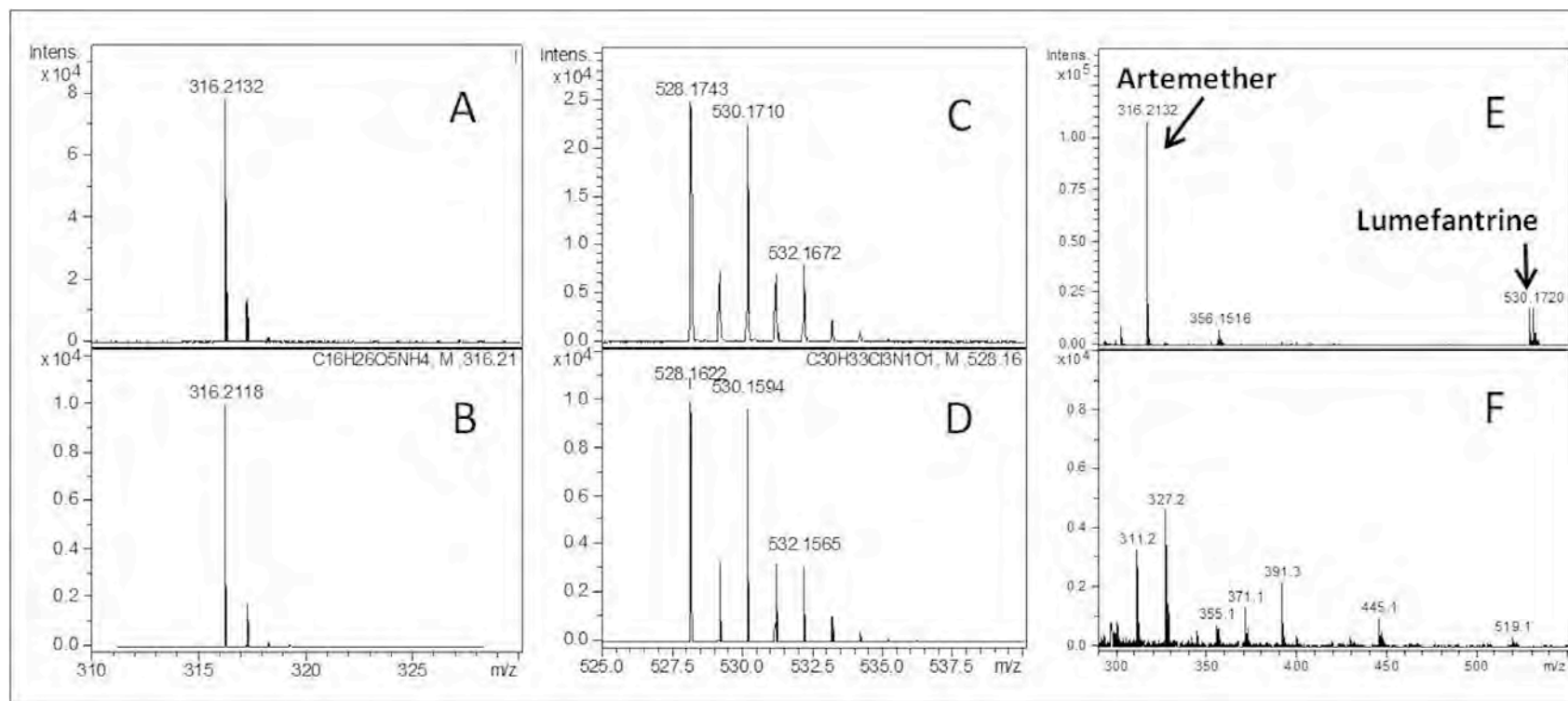


**Figure 4:** DART-MS and MS/MS analysis of sample tablet Ao-2012-2 in positive mode (left panels) and negative mode (right panels). A: Full mass spectrum, B: MS/MS spectrum of  $m/z$  283.1794 (polyethylene glycol), and C: MS/MS spectrum of  $m/z$  342.1454 (disaccharide), D: Full mass spectrum, and E: MS/MS spectrum of  $m/z$  763.1701 (pentasaccharide). Loss of 97.97 suggests the presence of phosphoric acid as an adduct with the pentasaccharide.

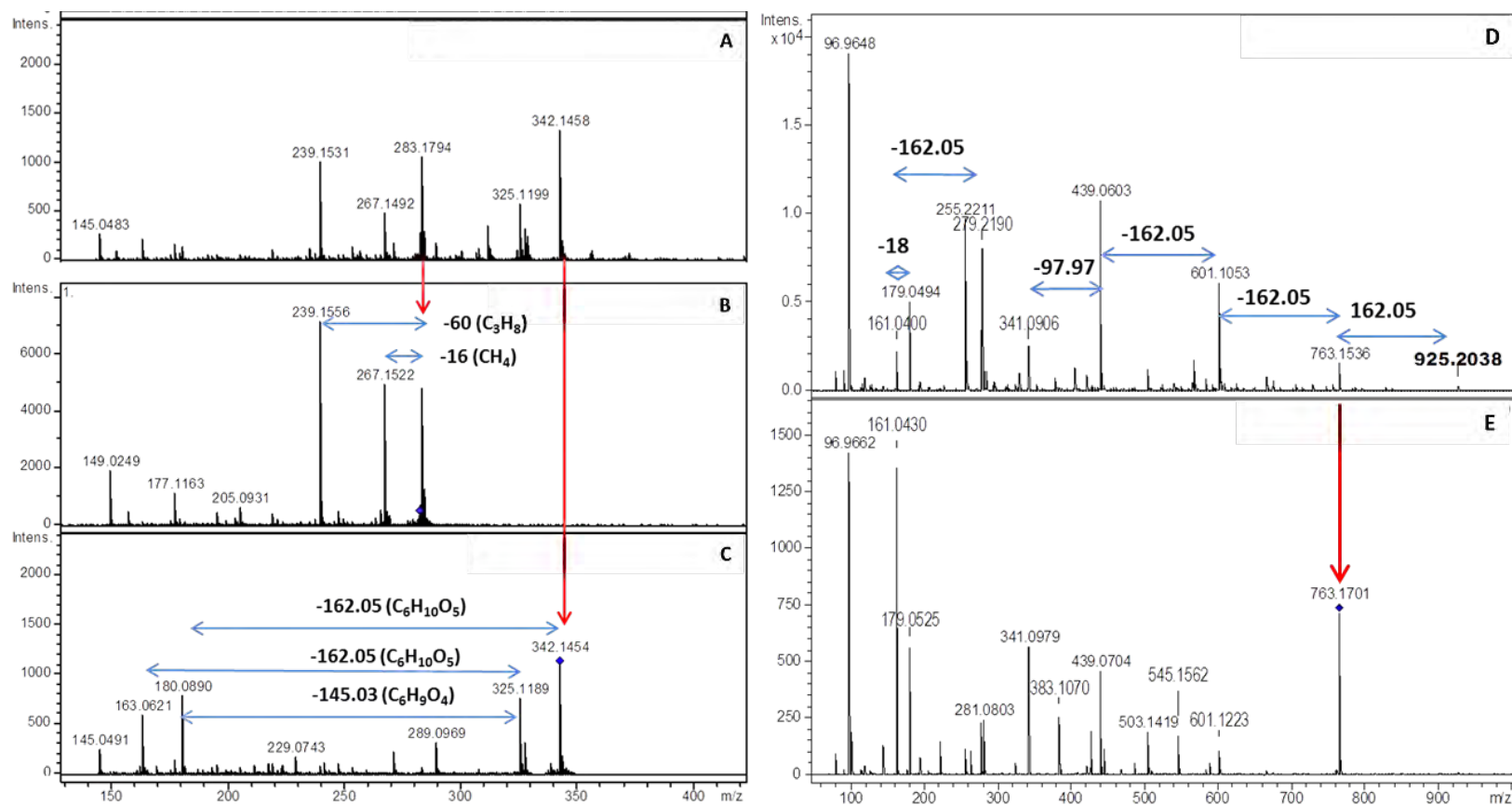


**Figure 4:** DART-MS and MS/MS analysis of sample tablet Ao-2012-2 in positive mode (left panels) and negative mode (right panels). A: Full mass spectrum, B: MS/MS spectrum of  $m/z$  283.1794 (polyethylene glycol), and C: MS/MS spectrum of  $m/z$  342.1454 (disaccharide), D: Full mass spectrum, and E: MS/MS spectrum of  $m/z$  763.1701 (pentasaccharide). Loss of 97.97 suggests the presence of phosphoric acid as an adduct with the pentasaccharide.

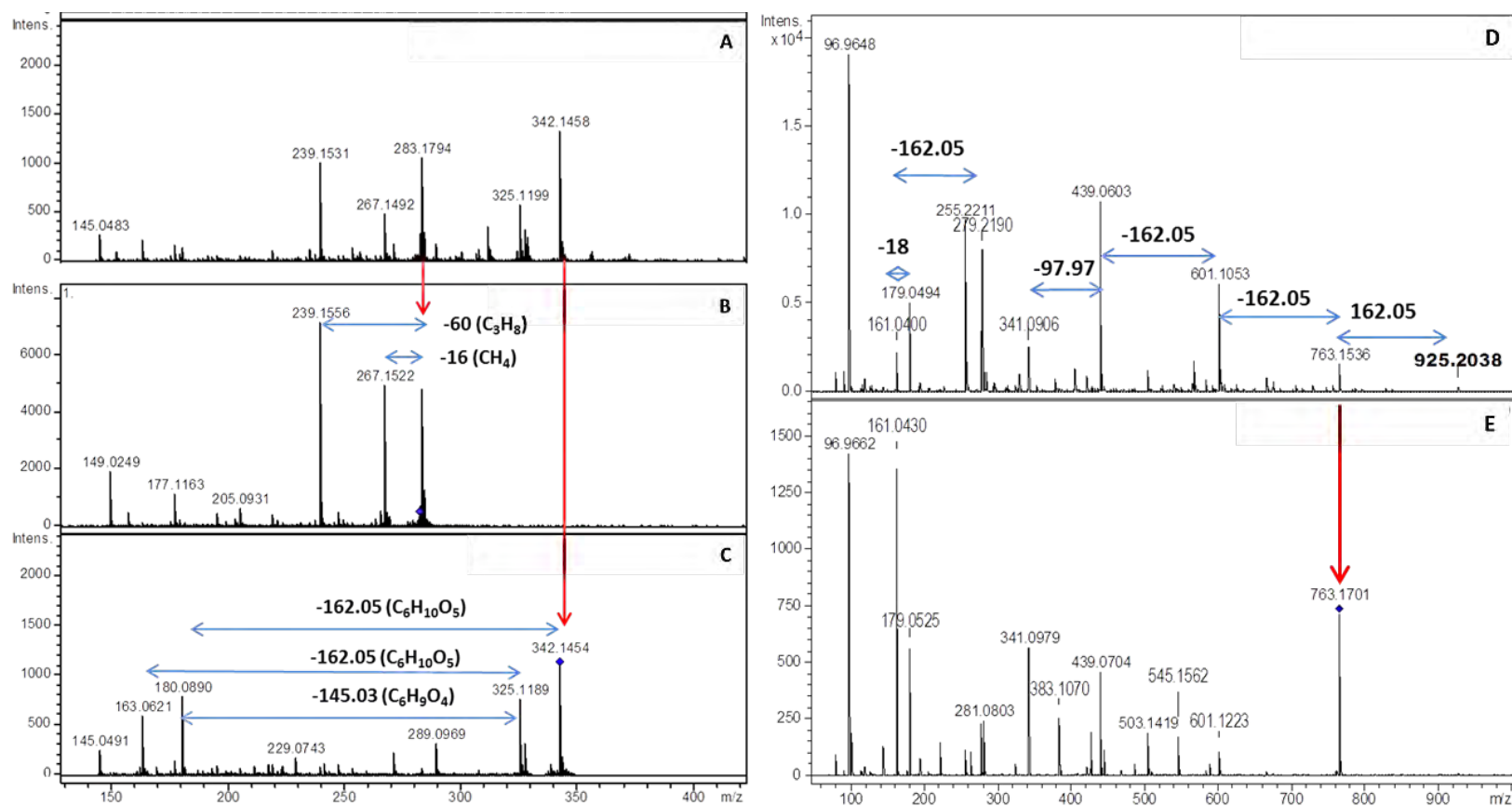


**Figure 5:** XRD scan of the of the sample tablet Ao-2012-2. XRD scan shows the s diffraction pattern (red) matches with brushite diffraction pattern (blue).

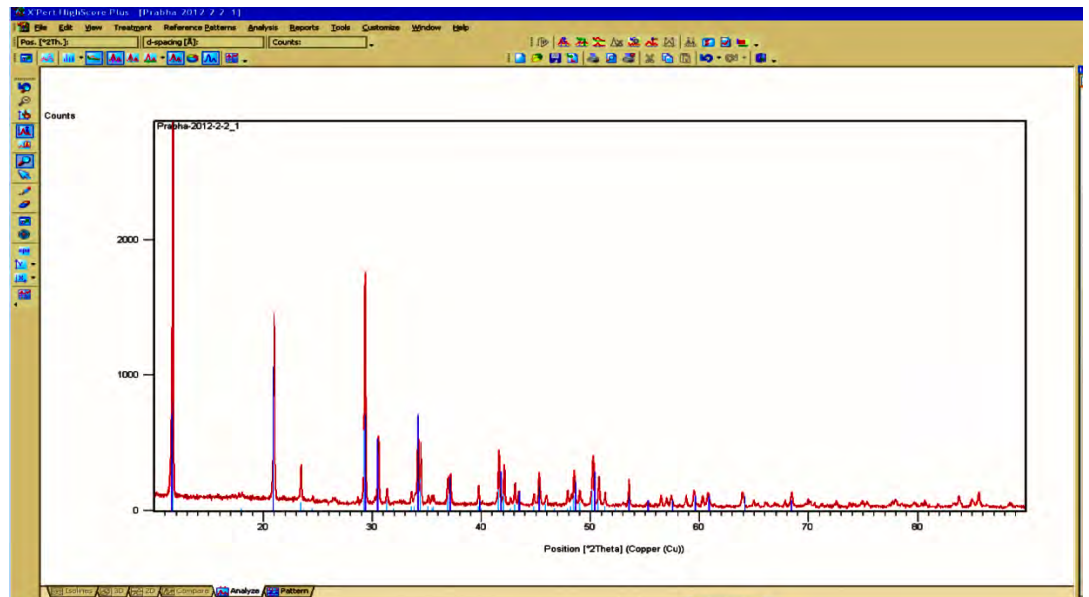
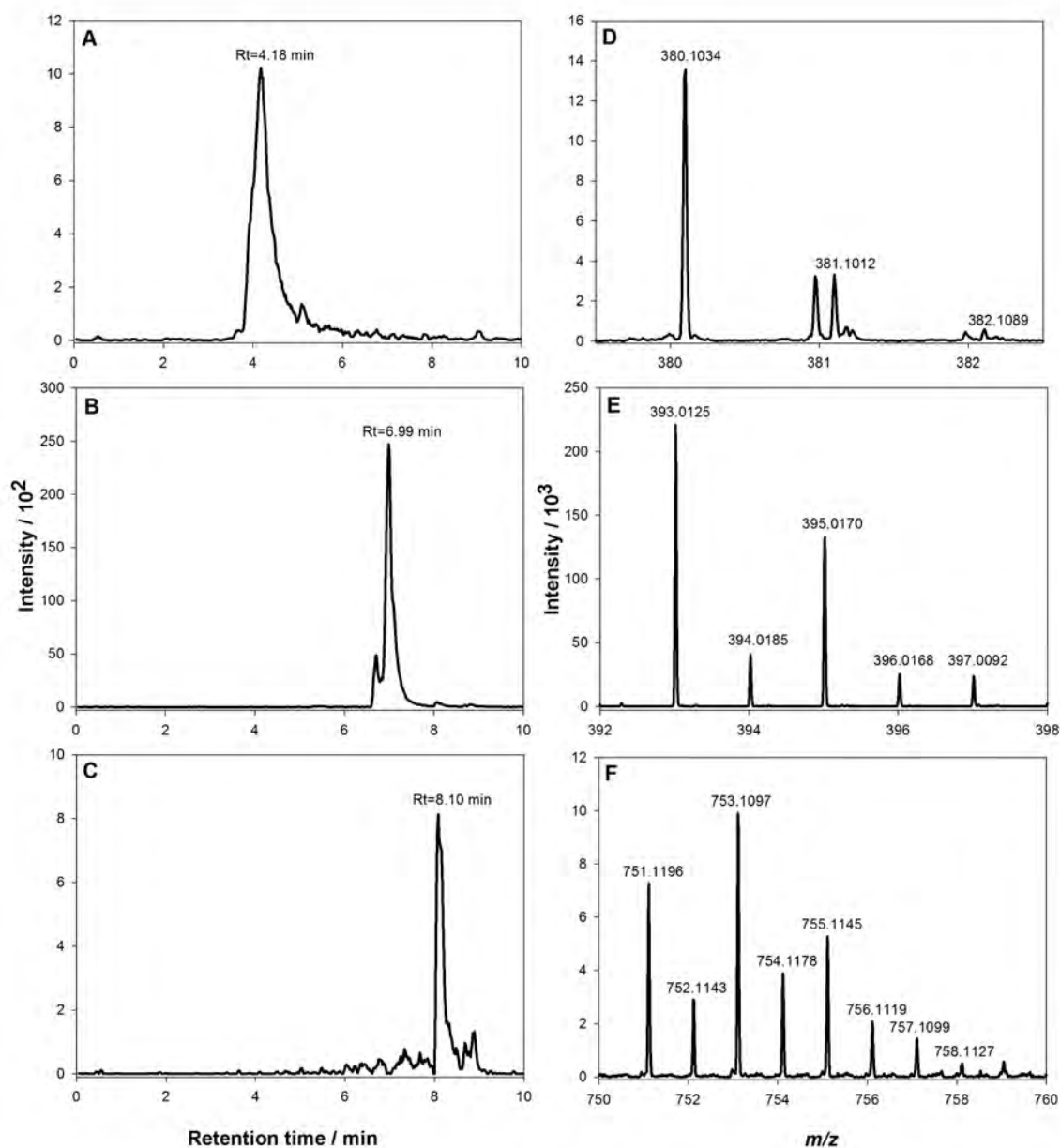


Figure 3: XRD scan of the of the sample tablet A0 2012-2. XRD scan showing the sample diffraction lines (red) matched with brushite diffraction lines (blue).

**Figure 6.** UHPLC-MS pigment analysis of Ao-2012-2. Extracted ion chromatogram for pigment 151 with  $m/z$   $380.0995 \pm 0.0050$  (A), pigment 3 with  $m/z$   $393.0157 \pm 0.0050$  (B), and pigment 81 with  $m/z$   $751.1161 \pm 0.0050$  (C). Mass spectra extracted from chromatographic peaks in the retention time range of 3.50-5.00 min for pigment 151 (D), 6.50-7.50 min for pigment 3 (E), and 8.00-8.50 min for pigment 81 (F).





**Figure 7.** Images captured by the CD-3. Genuine AMFm Coartem (top), falsified Coartem (Ao-2012-2) (bottom) under UV-Visible light demonstrating different background colours and red for '20/120'.





**Figure 8.** Images captured by the CD-3. Falsified AMFm Coartem (Ao-2012-2) (left), and genuine AMFm Coartem (right) demonstrating different tablet colours.

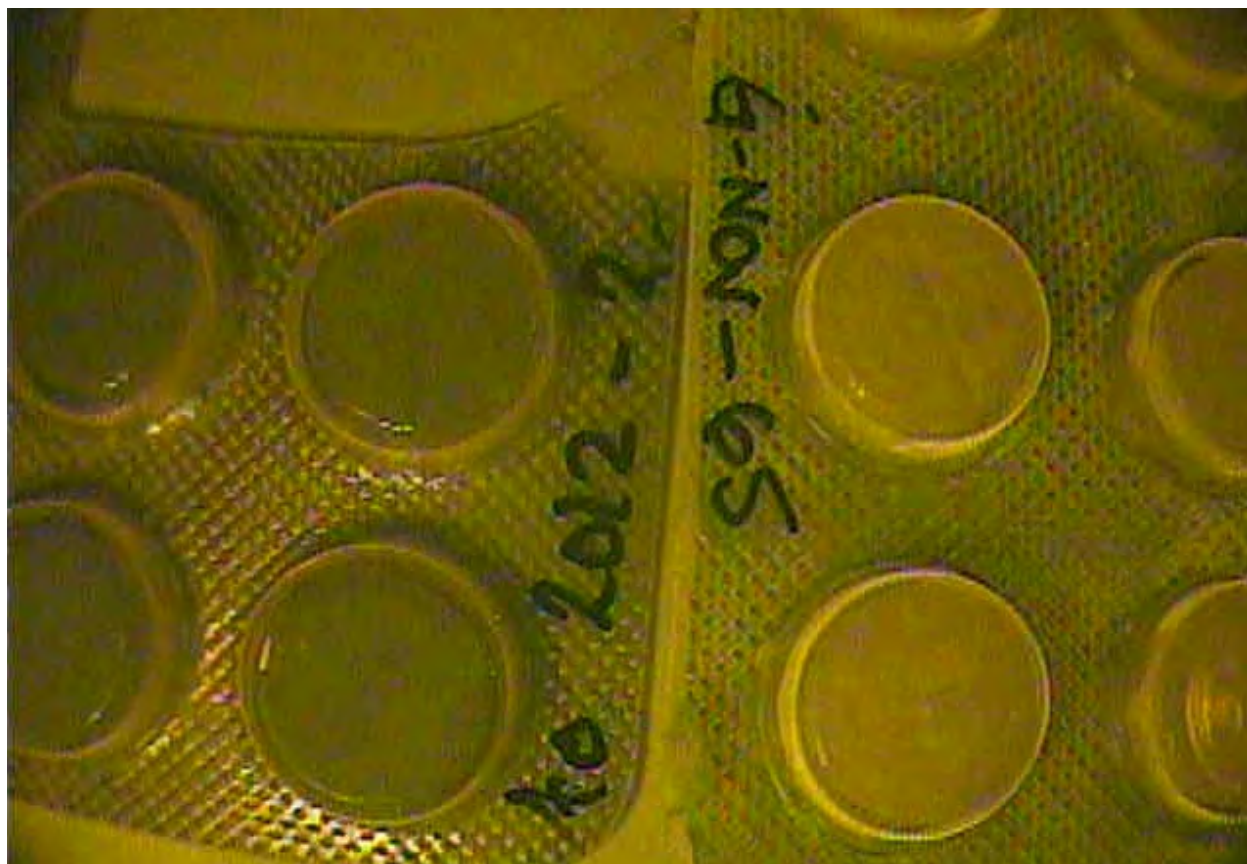


**Figure 9.** DART-MS and DART-MS/MS analysis of levamisole standard and suspect tablet. A) Fragmentation pattern of levamisole reported in the National Institute of Standards and Technology (NIST) database; B) Full mass spectrum of the levamisole standard with  $[M+H]^+$  at  $m/z$  205.0862 ( $\Delta m=6.3$  mDa); C) Product ion mass spectrum for the  $[M+H]^+$  precursor ion of levamisole at  $m/z$  205.0856 ( $\Delta m=5.7$  mDa) with a collision energy of 15 eV; D) Full mass spectrum of the suspect tablet Ao-2012-1; and E) Product ion mass spectrum for the  $[M+H]^+$  precursor ion at  $m/z$  205.0880 with a collision energy of 15 eV.

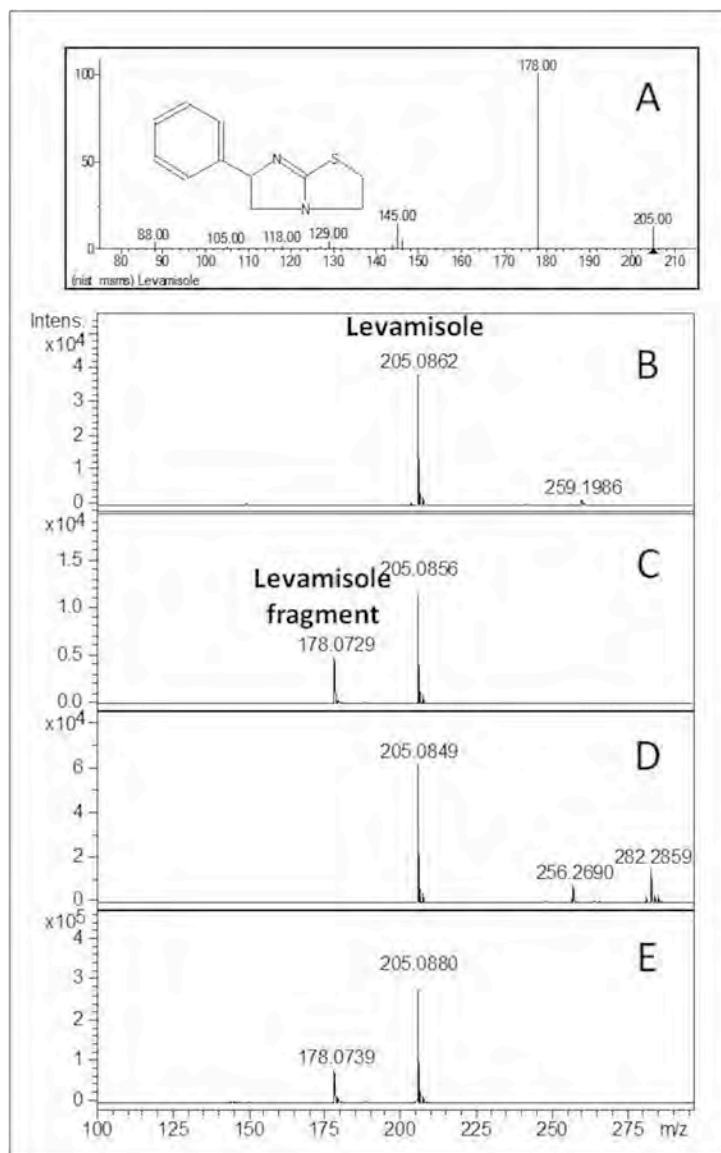


**Figure 10:** UHPLC-MS analysis of suspect tablet and standards of mebendazole and levamisole (Y-axis: intensity for all panels; X-axis (retention time in minutes for panels A, B, C, D, and E and  $m/z$  for panels A<sub>1</sub>, B<sub>1</sub>, C<sub>1</sub>, D<sub>1</sub>, and E<sub>1</sub>). Total ion chromatograms obtained of A: mebendazole; B and C: levamisole standard at two different concentrations; and D and E: suspect tablet at two different concentrations. Mass spectra extracted from chromatographic peaks in the retention time range of 1.9-2.25 min for A<sub>1</sub> and 1.11-1.35 min for B<sub>1</sub>, C<sub>1</sub>, D<sub>1</sub>, and E<sub>1</sub>. Theoretical masses of the  $[M + H]^+$  ions of mebendazole ( $C_{16}H_{13}N_3O_3$ ) and levamisole ( $C_{11}H_{12}N_2S$ ) are 296.1029 and 205.0799, respectively. Experimental  $m/z$  values measured for the standards of mebendazole and levamisole were 296.1014 and 205.0793, respectively.

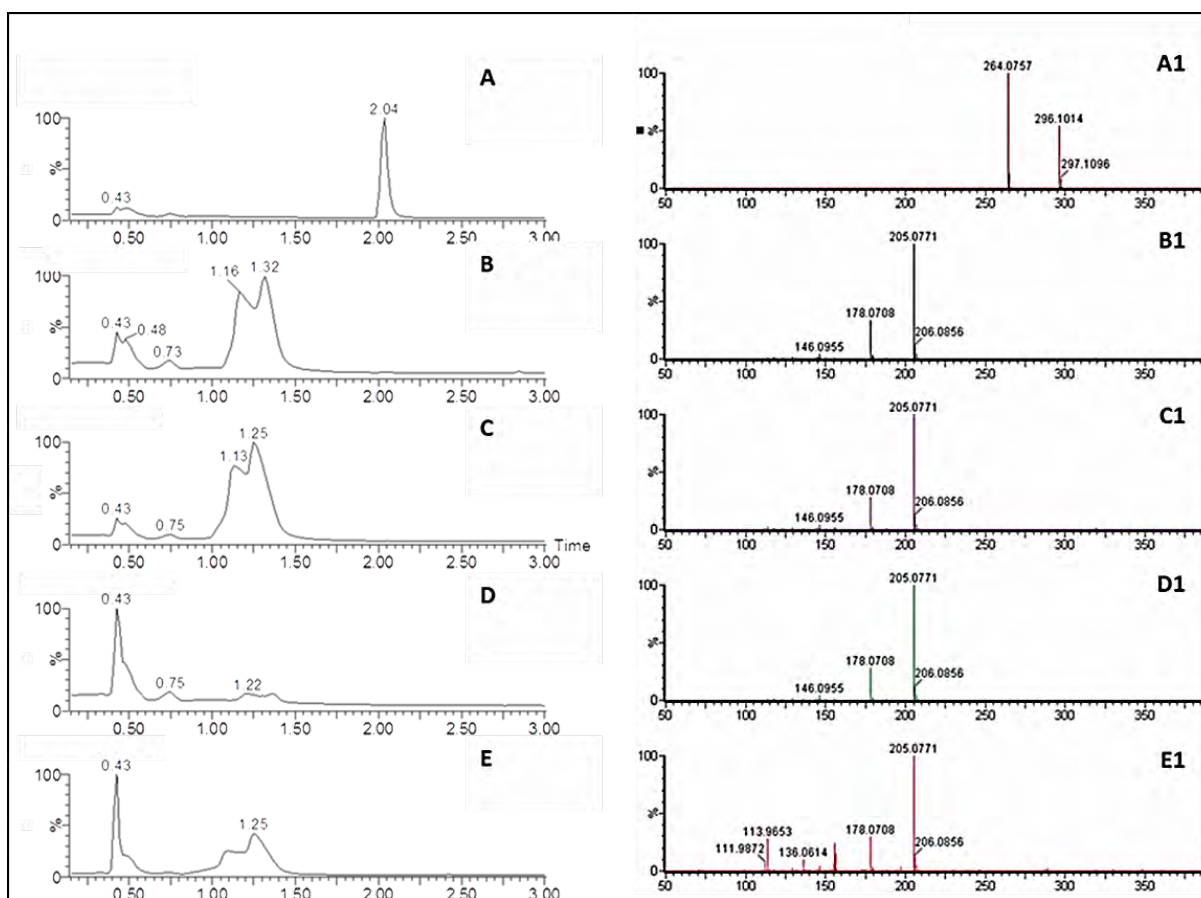


**Figure 11:** UHPLC-TWIMS-MS analysis of standard levamisole (left panel) and suspect tablet (right panel). Y-axis: Signal Intensity for all panels; X-axis: Retention time in minutes for panels A, B, A<sub>1</sub> and B<sub>1</sub>, and Drift time in milliseconds for panels C and C<sub>1</sub>. A and A<sub>1</sub>: extracted ion chromatogram at  $m/z$  205.0771  $\pm$  0.0050 corresponding to  $[M + H]^+$  ion of levamisole, B and B<sub>1</sub>: total ion chromatogram, C and C<sub>1</sub>: extracted ion mobility chronogram for the  $[M + H]^+$  ion of levamisole at  $m/z$  205.0771  $\pm$  0.0050.

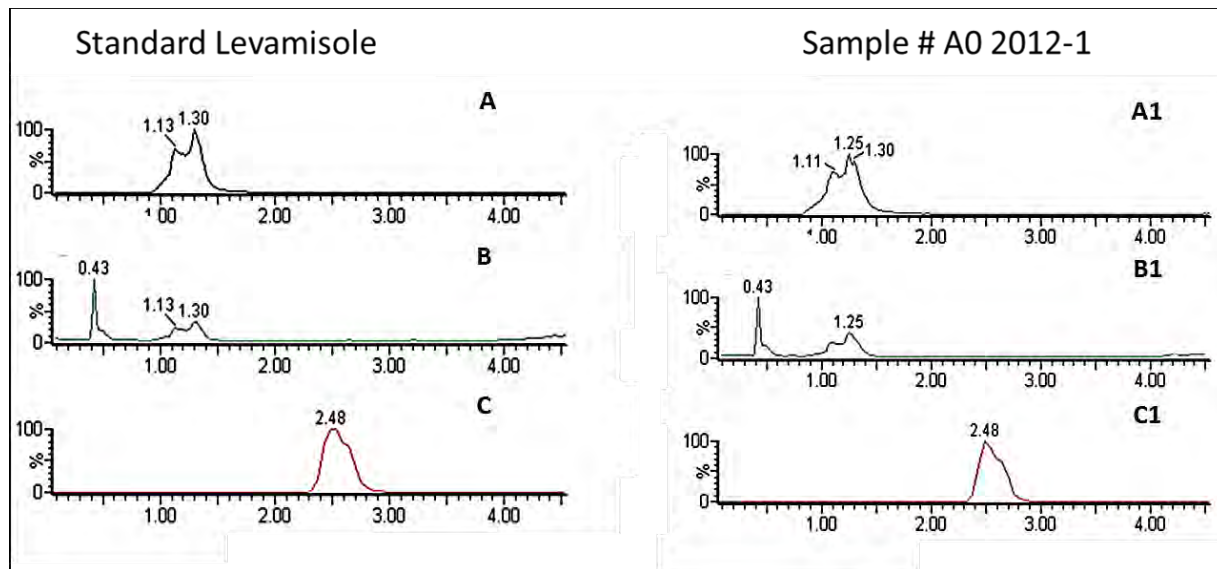


**Figure 12:** Calibration curve for the quantitation of levamisole present in the sample Ao-2012-1. Concentrations of the levamisole standards are shown next to the data points. To introduce a self check in the calibration curve a levamisole standard solution of 44 mM concentration was prepared from a stock solution different from the one used to prepare the dilutions along the calibration curve.

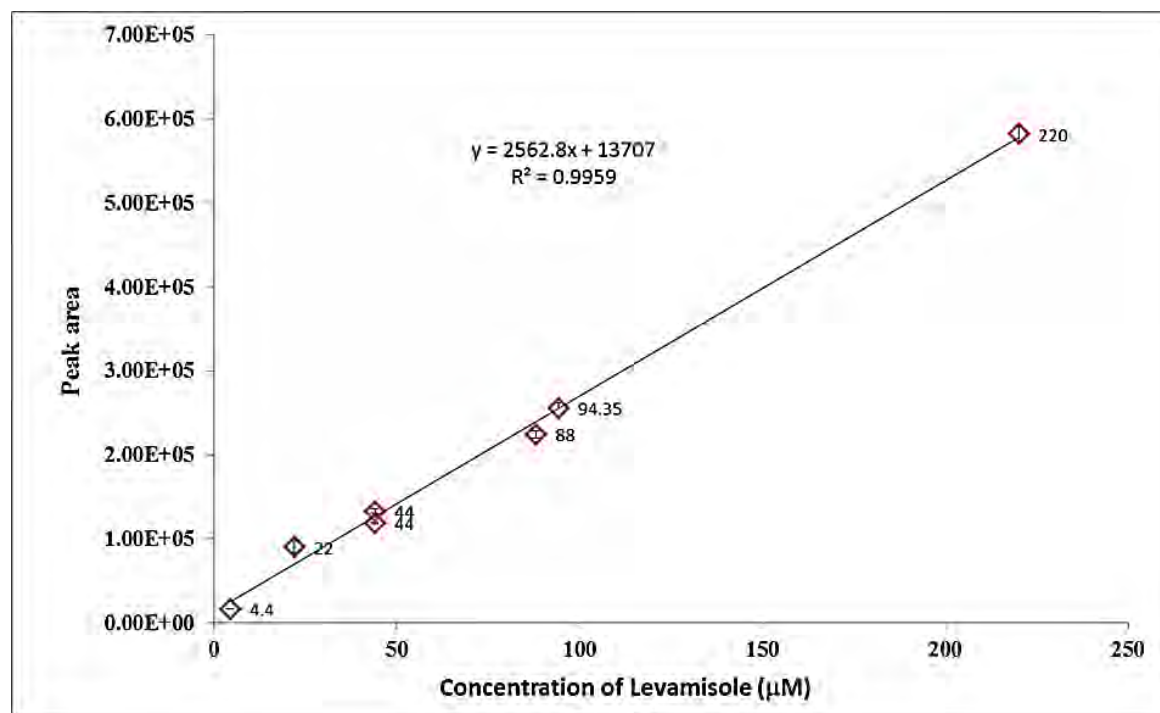


**Figure 13:** Negative mode DART-MS analysis (left panel) and XRD scan (right panel) of the of the sample tablet Ao-2012-1. A) full DART-MS spectrum of the sample, B) MS/MS spectrum of the precursor ion at  $m/z$  359.0762, and C) XRD scan showing that the sample diffraction pattern (red) matches with calcite diffraction pattern (blue).

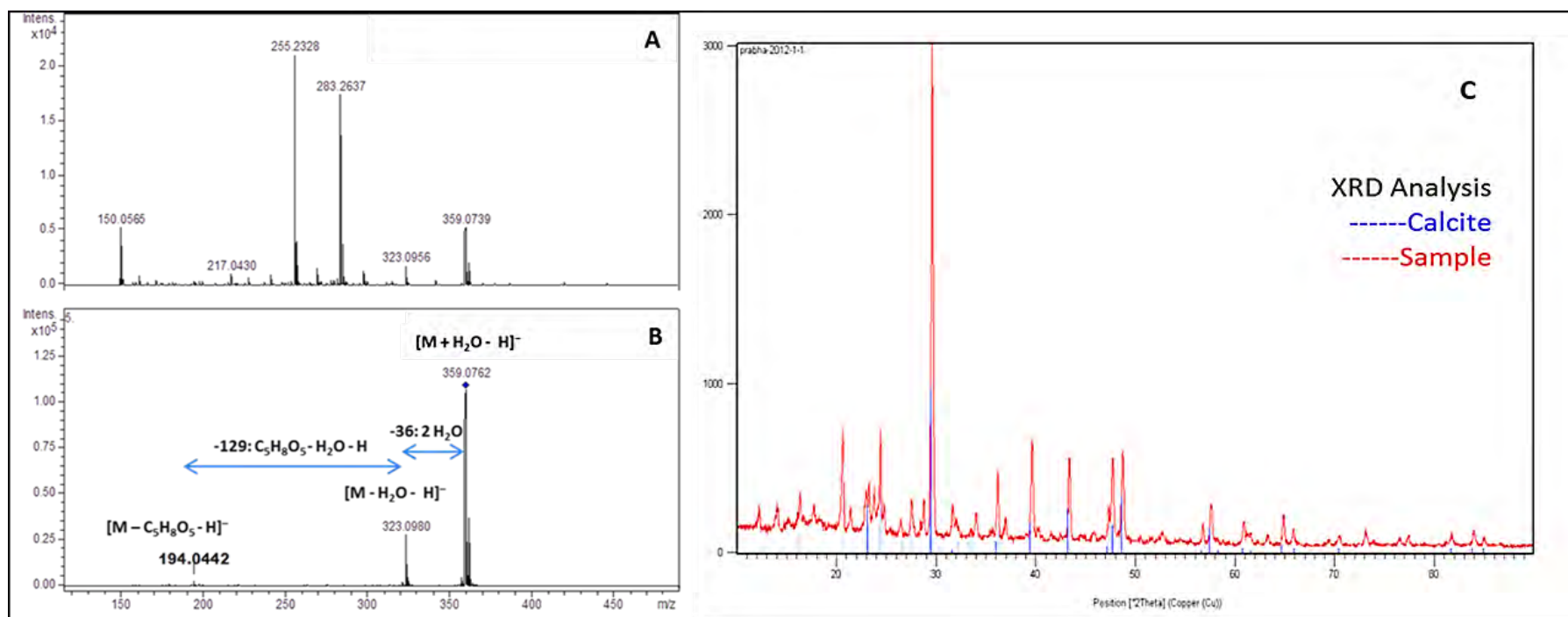


**Figure 14.** Images captured by the CD-3. Falsified mebendazole (Ao-2012-1) (left), genuine mebendazole (right), demonstrating different colours, under UV-Visible light for the centre on the box packaging.

